33rd Annual International Conference of the IEEE EMBS
Boston, Massachusetts USA, August 30 - September 3, 2011

Robotic Endoscope Motor Module and Gearing Design

Jillian M. Oliveira, Yi Chen, and Ian W. Hunter

Abstract— **Actuation of a robotic endoscope with increased torque output is presented. This paper will specifically focus on the motor module section of a robotic endoscope, which comprises of a pair of motors and gear reduction assemblies. The results for the endoscope and biopsy tool stiffness, as well as the stall force and force versus speed characteristics of the motor module assembly are shown. The scope stiffness was found to be 0.006 N/degree and additional stiffness of the biopsy tools were found to be in the range of 0.09 to 0.13 N/degree. Calculations for worm gearing and efficiency are discussed.**

I. Introduction

ENDOSCOPES are widely used for diagnostic purposes, but endoscopic procedures tend to involve biopsies to remove tissue for further examination. Therefore, an endoscope needs to be able to successfully control the motion of not only the endoscope, but any tools that are inserted within it for these types of procedures. The biopsy tools presented here are much stiffer than the scope, and thus, endoscopes need to account for this additional stiffness when designing the actuation method for turning. By focusing specifically on the mechanics of the motor module section of the proposed endoscope, this paper proposes ways of increasing the torque to turn the inserted biopsy tool with the rest of the endoscope.

The endoscope design without the extra worm gearing [1] can achieve a full 360 degrees of motion, but lacks the torque to pull a stiffened scope through this full motion when a biopsy tool is inserted. The goal of the presented motor module is to increase the pulling force to ease the bending of the stiffened scope. To achieve this, the motor module section and appropriate gearing was adjusted.

The proposed motor module section comprises of a DC motor with 25:1 planetary gearbox. The output shaft of the motor and gearbox is coupled to a worm gear, which drives the worm wheel and shaft rotation. The reduction of the worm assembly is 23:1. This gear train results in a total 575:1 gear reduction. This large reduction aims to supply the torque needed to pull a stiffened scope and biopsy tool. A stiff motor module surrounds and holds the motor. It also bears the worm gear shown in Fige 1. Additional brass bearings were added for the tip of the worm gear and shaft. E-clips were used to constrain the shaft to only rotation.

Manuscript received June 20, 2011 for the IEEE EMB Conference

J. M. Oliveira, Y. Chen, and I. W. Hunter are with the Department of Mechanical Engineering at Massachusetts Institute of Technology, Cambridge, MA, 02139 U. S. A. (email: jilliano@mit.edu)

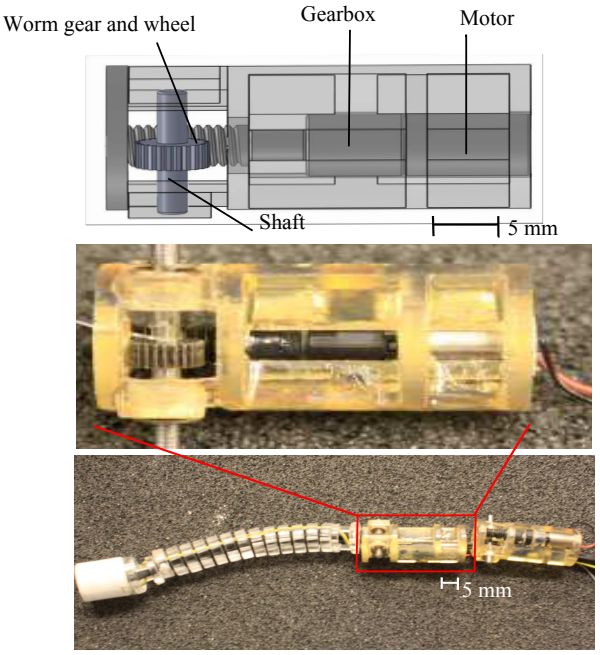

Fig. 1. Motor module section and corresponding CAD model without the outer sheath

II. Background Review

More generally, the modular endoscope is comprised of many parts. Beginning at the distal end of the endoscope, there is a tip module, comprising of a camera, LED lights, as well as the tip of the biopsy tool and any other necessary features needed for control. The turning section is comprised of many circular turning modules, which is actuated by control strings via the motor module section. The motor module section, as described previously, is followed by a variably stiff body section [1]. The endoscope is surrounded by an outer sheath and sterilized for single use. The overall system is shown at the bottom of Figure 1.

The tip is actuated from the motor module section by monofilament cables, which attach to the shaft. As the shaft turns in one direction, one monofilament wraps around the shaft, shortening the length of one cable and the other cable unwraps, lengthening the other cable. This turns the endoscope 180 degrees along two cardinal directions. Another motor module section is placed directly behind the first. When rotated 90 degrees around the central axis of the endoscope, with the same approach, this module will move the endoscope in the last two cardinal directions. Together,

a full 360 degrees of motion is achieved [1].

For increasing the torque of the motors to turn a stiffened tip section, gear reduction is a clear choice. Worm gears [2] are favorable over other gearing or lead screw options [3], [4], as the worm gears will provide a high gear ratio with fewer gears within a smaller space. In addition, worm gears are not back-drivable which can protect the motor and gearbox. On the other hand, worm gears can have low efficiencies depending on the arrangement of the gear angles and the materials used for the gear.

Other options to create a turning tip, such as shape memory alloys [5], [6], [7] require more longitudinal space within the endoscope length. Pneumatic [8], [9] turning methods require additional air lines bladders and valves.

The incidence of hospitalizations from damage or infection to the colon during endoscopies [1], [10] can be addressed by carefully designed single-use robotic systems. In order to be useful for endoscopic procedures, however, endoscopic tools, such as disposable forceps or cauterizers need to be inserted and positioned by the tip. This requires a strong, compact, low cost, and disposable endoscope tip system. This strategy is distinct from other systems where non-standard roboticized tools cannot be easily swapped out or disposable [11].

III. Theory and Design

In the design of worm gears, maximizing efficiency with the designated torque is important. The following equations are based on the geometry of the worm gear and wheel and conclude with the appropriate gear efficiency of a worm assembly [12].

The tangential force on worm, F_{wt}, can be calculated from a basic torque equation, by dividing the worm torque by the pitch radius,

$$F_{wt} = \frac{2M_1}{D_1}, \tag{1}$$

where M_1 is the worm torque and D_1 is the pitch diameter of the worm.

The tangential force on the worm gear, F_{gt} can be calculated by

$$F_{gt} = F_{wt}\frac{\cos\alpha_n - \mu\tan\gamma}{\cos\alpha_n\tan\gamma + \mu}, \tag{2}$$

where μ is the coefficient of friction, α_n is the normal pressure angle (deg), and γ is the worm lead angle (deg). For worm gears, α_n is commonly 20 degrees.

The output torque, M_2, is then found by multiplying the pitch radius of the worm wheel by the tangential force of the worm wheel, another torque equation,

$$M_2 = F_{gt}\frac{D_2}{2}, \tag{3}$$

where D_2 is the pitch diameter of the worm wheel. Note that the coresponding forces and diameters of the worm design are shown in Figure 2.

The efficiency of the worm assembly can range from 20% to close to 100% based on the geometry of the worm gear and wheel. The efficiency, η, can be calculated by diving the output torque with friction by the output torque without friction, yielding,

$$\eta = \frac{\cos\alpha_n - \mu\tan\gamma}{\cos\alpha_n + \mu\cot\gamma}. \tag{4}$$

Given that a normal pressure angle (α_n) for worm gears is 20 degrees, given low coefficients of friction, an optimal worm lead angle (γ) to optimize efficiency is between 40 and 50 degrees. Assuming a coefficient of friction value of 0.3, the calculated efficiency for the worm gears is 56%. Additionally, materials that can be used to reduce friction include hardened steel for the worm gear and phosphor bronze for the worm wheel. These materials are strong enough such that the gear teeth will not fail under load [12]. The current motor module worms and worm gear are made from hardened steel and 4042 steel respectively. The worm gear was cut on an electric discharge machine (EDM). The motor module bearings are made of brass and are encased by Acura 40 stereolythography material. The case can also be injection molded for cost. The motors used are low-cost gear head motors with a diameter of 6 mm. There is a tool passage that is 4 mm in diameter within the casing. The motor module is a maximum of 14 mm in diameter, but can be simply scaled smaller with improved manufacturing methods.

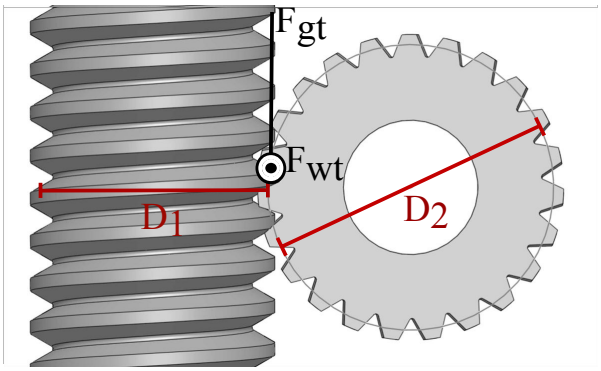

Fig. 2. Geometry and tangential forces of worm gear and wheel

IV. Results

Several results were collected for endoscope. First, stiffness of the endoscope turning section was measured - without as well as with two different biopsy tools. The results of the scope stiffness with and without biopsy tools are plotted in Figure 3a. The scope stiffness was found to be 0.006 N/degree and additional stiffness of the biopsy tools were

found to be in the range of 0.09 to 0.13 N/degree. Units of N/degree are used because the axis of rotation is not defined in the endoscope system. The scope length is approximately 60 mm, an appropriate length for the turning section. Other lengths were measured (not pictured) but a general trend was observed. In order to achieve a higher angle, a higher force is necessary.

Without the biopsy tool, the force needed to turn the endoscope 180 degrees is significantly less than when a biopsy tool is inserted, hence the need for the worm assembly. It is noted that the Pentax forceps, which is made of a more flexible coiled spring, is less stiff than the Boston Scientific forceps, made mostly of stiffer plastic.

Now focusing specifically on the motor module section and the performance of the gear assembly, stall force and force versus speed characteristics were measured. In Figure 3b, the output stall force of the motor and gear assembly as a function of pulling force on the monofilament cables is plotted. The addition of the worm assembly shows an increase in the stall force over the motor and gearbox alone.

However, this increase is much less than expected. The results show only a 1.5× increase in force, but from an extra 23:1 gear ratio; there should be a 23× increase in force. There is a lot of power lost, but there are a few reasons to explain this. The manufacturing of the worm wheel can be done with more precision and detail in the future, which will result in a cleaner interaction between the worm wheel and the worm gear. A stiffer motor module and coupling between the shaft of the motor and the worm gear may also help with the power lost to poor alignment. Another future goal is to decrease the friction between the gears, which will help decrease the losses.

The plot of output speed as a function of pulling force for various voltages is shown in Figure 3c. These results show a general and expected trend. The speed per unit force is much lower with the additional worm gears than it was with the gearbox and motor alone. The trend also decreases with decreasing voltage.

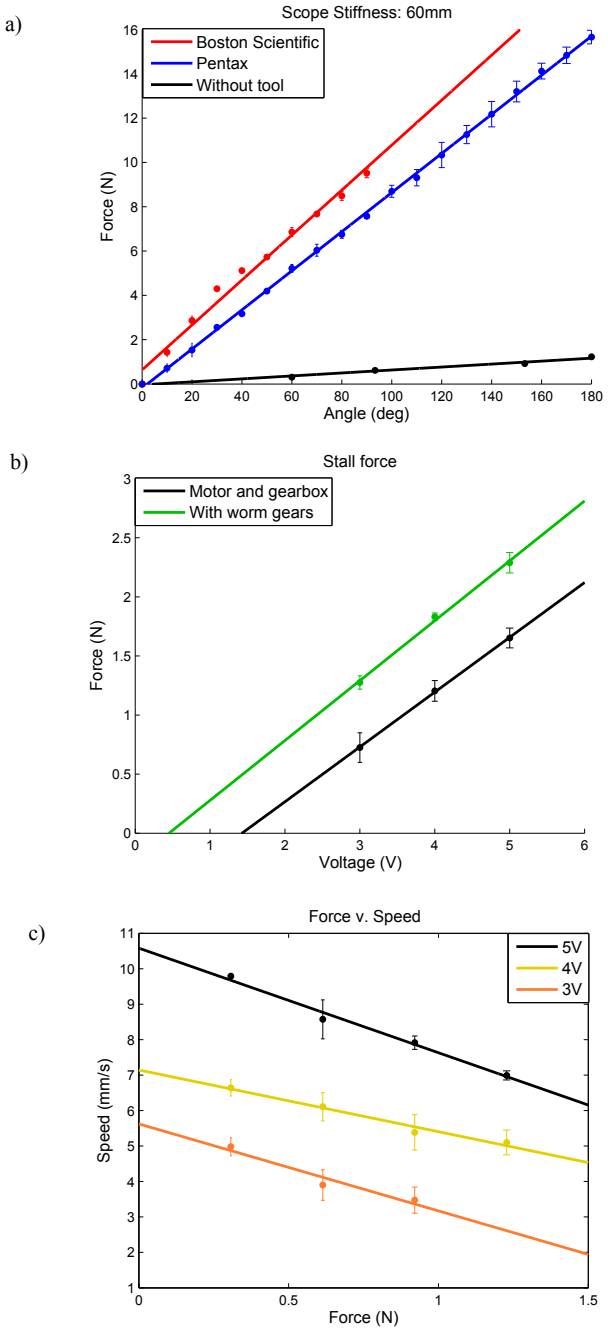

Fig. 3. a) Experimental bending angle of the scope (60 mm in length) with and without a biopsy tool inserted as a function of pulling force. Two biopsy tools were used, Boston Scientific's Radial Jaw and Pentax forceps b) Experimental stall force as a function of voltage. With and without worm assembly was measured. c) Experimental stall speed as a function of pulling force for different voltages. Note that lines are linear least squares fits of the data collected.

V. Conclusion

Based on these results, we can turn the forceps through a full 180 degrees of motion when the stall force of the motor and gear assembly exceeds 16 N. Currently, we can turn the endoscope by about 180 degrees when there are no forceps and at least 20 to 40 degrees when there are forceps inside the endoscope tool passage. By adding the worm gear, we were able to increase the output force by 0.5 N. With the optimization in from the theory, we should be able to increase the force beyond the 16 N force necessary to turn the endoscope tip through the full motion. Future work includes optimizing efficiency though gear geometry, material selection, and bearing material selection.

A robotic endoscope with the ability to turn with forceps inside the tool passage is an important step to making robotic endoscopes a reality in clinical applications.

VI. Acknowledgment

The authors would like to thank Bryan Ruddy for his advice on manufacturing and Dr. Cathy Hogan for her help in

sourcing materials. This project would not have been possible without their help. We would also like to thank Shigehiko Tanaka and Al Couvillon for their early work on the project.

REFERENCES

[1] Y. Chen, S. Tanaka, and I. W. Hunter, "Disposable endoscope tip actuation and robotic platform," in *32nd Annual Interational Conference of the IEEE Engineering in Medicine and Biology Society*, pp. 2279–2282, 2010.

[2] J. Peirs, D. Reynaerts, and H. V. Brussel, "A miniature manipulator for integration in a self-propelling endoscope," *Sensors and Actuators A*, vol. 92, pp. 343–349, 2001.

[3] K. Wang, G. Yan, G. Ma, and D. Ye, "An earthworm-like robotic endoscope system for human intestine: Design, analysis, and experiment," *Annals of Biomedical Engineering*, vol. 37, no. 1, pp. 210–221, 2009.

[4] H. Ueno, Y. Ikeda, T. Sato, and S. Nakamura, "Endoscope," U.S. Patent 7,780,593 Aug 24, 2010.

[5] J. Peirs, D. Reynaerts, and H. V. Brussel, "Design of a shape memory actuated endoscope tip," *Sensors and Acutators A*, vol. 70, pp. 135–140, 1998.

[6] J. M. Stevens and G. D. Buckner, "Actuation and control strategies for miniature robotic surgical systems," *Dynamic Systems, Measurement, and Control*, vol. 127, pp. 537–549, 2005.

[7] J. Peirs, D. Reynaerts, and H. V. Brussel, "A micro robotic arm for a self propelling colonoscope," in *Proceedings of the 6th International Conference on New Actuators*, vol. 98, pp. 576–579, 1998.

[8] A. Menciassi, J. H. Park, S. Lee, S. Gorini, P. Dario, and J. Park, "Robotic solutions and mechanisms for a semi-autonomous endoscope," in *Proceedings of the International Conference on Intelligent Robots and Systems*, pp. 1379–1384, 2002.

[9] D. Glozman, N. Hassidov, M. Senesh, and M. Shoham, "A self- propelled inflatable earthworm-like endoscope actuated by single supply line," *IEEE Transations on Biomedical Engineering*, vol. 57, no. 6, pp. 1264–1272, 2010.

[10] D. A. Leffler, R. Kheraj, S. Garud, N. Neeman, L. A. Nathanson, C. P. Kelly, M. Sawhney, B. Landon, R. Doyle, S. Rosenberg, and M. Aronson, "The incidence and cost of unexpected hospital use after scheduled outpatient endoscopy," *Archives of Internal Medicine*, vol. 170, no. 19, pp. 1752–1757, 2010.

[11] M. Tavakoli, R. V. Patel, and M. Moallem, "Haptic interaction in robot-assisted endoscopic surgery, a sensorized end-effector," *International Journal of Medical Robotics and Computer Assisted Surgery*, vol. 1, no. 2, pp. 53–63, 2005.

[12] "Worm gears." Electronic, `http://www.roymech.co.uk/Useful_Tables/Drive/Worm_Gears.html`, April 2010.